Supporting Info

Revising the role of chromium on the surface of perovskite electrodes: poison or promoter for the solid oxide electrolysis cell performance?

Dingkai Chen,[a] Basma Mewafy,[a] Fotios Paloukis,[a,b] Liping Zhong[a], Vasiliki Papaefthimiou[a], Thierry Dintzer[a], Kalliopi M. Papazisi,[c] Stella P. Balomenou,[c] Dimitrios Tsiplakides,[c,d] Detre Teschner,[e,f] Virginia Pérez-Dieste,[g] Carlos Escudero,[g] and Spyridon Zafeiratos,[a,*]

[a]*Institut de Chimie et Procédés pour l'Energie, l'Environnement et la Santé, UMR 7515 du CNRS-UdS 25 Rue Becquerel, 67087 Strasbourg, France*
[b]*Foundation for Research and Technology, Institute of Chemical Engineering Sciences (FORTH/ICE-HT), Patras, GR-26504, Greece*
[c]*Chemical Process and Energy Resources Institute /CERTH, 6th km Charilaou-Thermi Rd., 57001 Thessaloniki, Greece*
[d]*Department of Chemistry, Aristotle University of Thessaloniki, 54124 Thessaloniki, Greece*
[e]*Departement of Inorganic Chemistry, Fritz-Haber-Institut der Max-Planck-Gesellschaft, Faradayweg 4-6, 14195 Berlin, Germany*
[f]*Department of Heterogeneous Reactions, Max-Planck-Institut für Chemische Energiekonversion, Stiftstrasse 34-36, 45470 Mülheim a. d. Ruhr, Germany*
[g]*ALBA Synchrotron Light Source, Carrer de la Llum 2-26, Cerdanyola del Vallès, 08290 Barcelona, Spain*

Supporting information 1

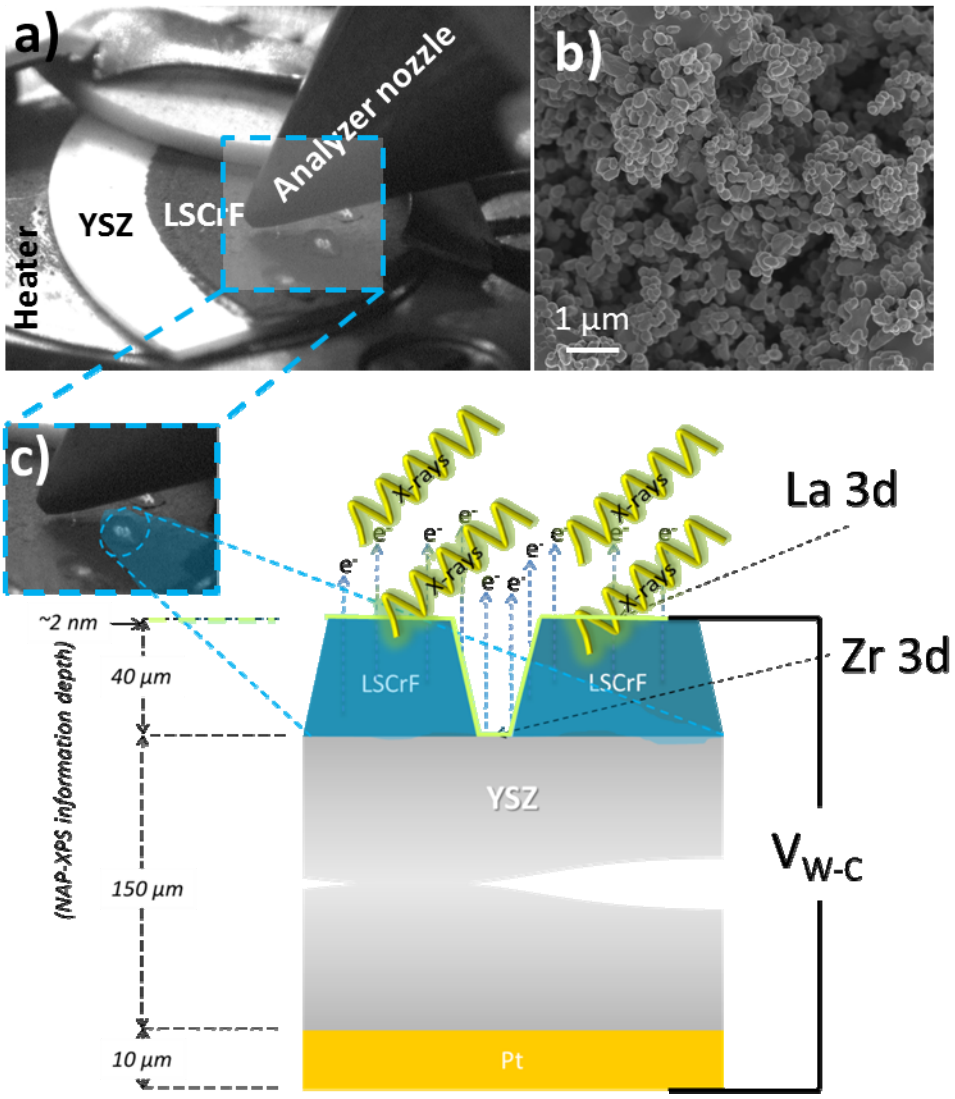

Figure S 1. a) Photograph of the NAP-XPS sample holder with the mounted LSCrF sample. b) SEM micrograph of the top side of the electrode which is characteristic of the surface morphology c) schematic representation of the electrolytic cell including the dimensions of the cell and the analysis depth probed by NAP-XPS. Please note that Zr 3d measurements are not discussed here.

Supporting information 2

The information depth of XPS depends on 3 main factors; the material, the kinetic energy of the measured photoelectrons and the angle θ between the sample surface normal and the analyzer (emission angle). In homogenous materials, in a first approximation, the intensity contribution from a depth *d* is given, by the Beer-Lambert law :

$$I_{(d)}=I_{(d=0)}(1-e^{(-d/\lambda\cdot\cos\theta)}) \qquad \text{(eq. 1)}$$

where $I_{(d)}$ and $I_{(d=0)}$ is the number of electrons produced in a depth d and at the outermost surface (d=0), respectively. λ is the average inelastic mean free path (IMFP) of the photoelectrons, which depends on the material and the kinetic energy of the measured photoelectron. The λ value is

typically calculated using the so called TPP2M formula[1]. In the present work the average λ for the different components of the LSCrF was estimated about 0.67 nm (for 190 eV KE energy). Using equation 1 one can calculate that 95 % of the photoelectron signal ($I_{(d)}/I_{(d=0)}$=0.95) will come from a depth : $d \sim 3 \cdot \lambda \cdot \cos\theta$ (eq. 2)

This can be also considered as the typical information depth of XPS analysis. Taking into account that the angle between the surface normal and the analyzer is 50 degrees for CIRCE and 0 degrees for ISISS set ups, the information depth for CIRCE is calculated 3·0.67·cos50 nm= 1.29 nm and for ISISS 3·0.67·cos0 nm= 2.01 nm.

Supporting information 3

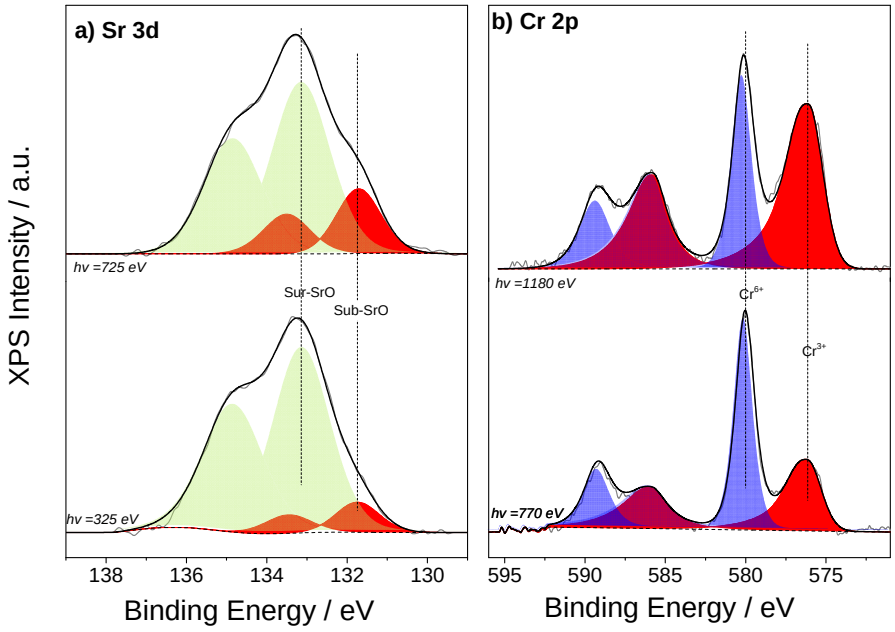

Figure S 2. Depth profiling NAP-XPS spectra from the LSCrF electrode recorded by using 2 different incident photon energies (*hv*) as indicated in the figure **a)** Sr 3d peak after annealing at 450 °C for 10 min in 0.5 mbar H_2O and **b)** Cr 2p peak after annealing at 890 °C for 10 min in 0.5 mbar O_2. All specrta were recorded after cooling down the sample at 350 °C

[1] QUASES-IMFP-TPP2M Ver 2.2

Supporting information 4

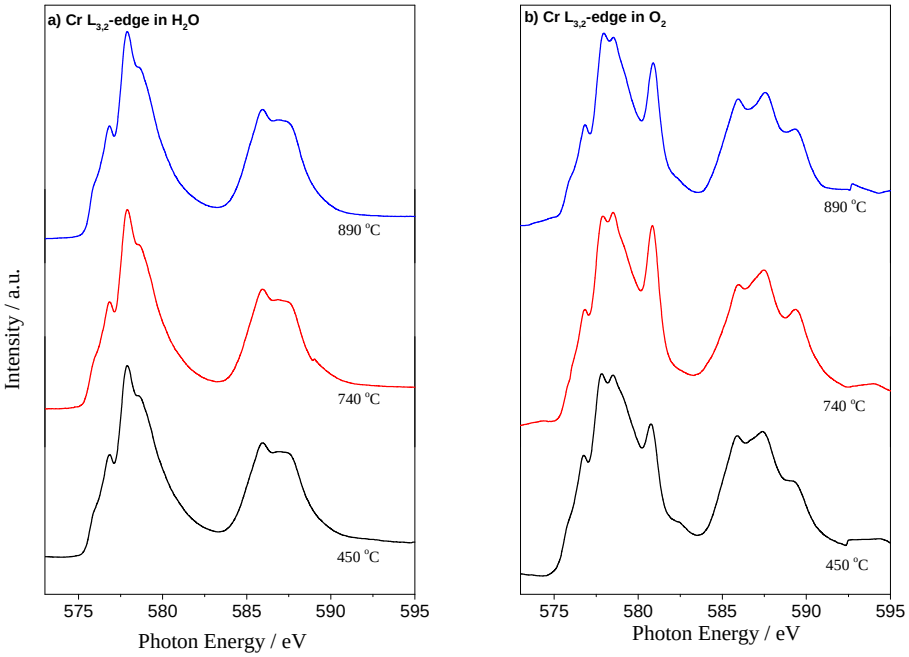

Figure S 3. Cr $L_{3,2}$-edge TEY-NEXAFS spectra recorded on the LSCrF electrode after annealing at the temperature indicated in the graph in (a) H_2O and (b) O_2 atmospheres.

Supporting information 5

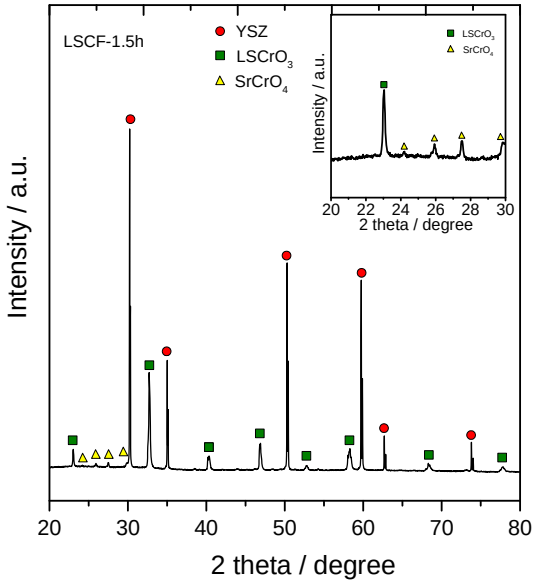

Figure S 4. XRD pattern of the LSCrF electrode recorded at room temperature after treatment in O_2 atmosphere. The inset shows the magnified 2 theta range where the main diffraction lines of $SrCrO_4$ are expected.

Supporting information 6

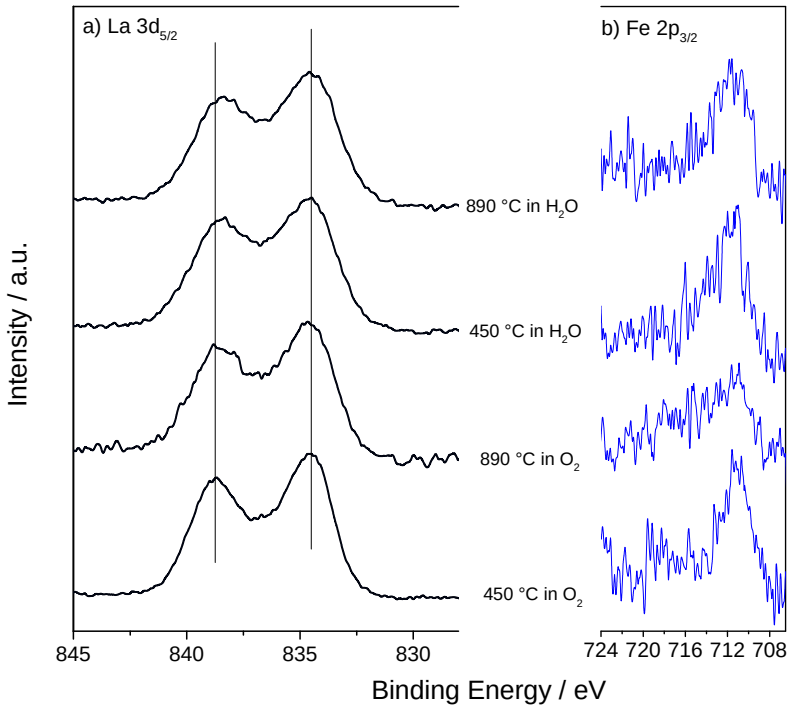

Figure S5. (a) La $3d_{5/2}$ (hν = 1030 eV) and (b) Fe 2p (hν = 900 eV) NAP-XPS spectra recorded on a LSCrF electrode after annealing for 10 min at the conditions indicated in the figure.

Supporting information 7

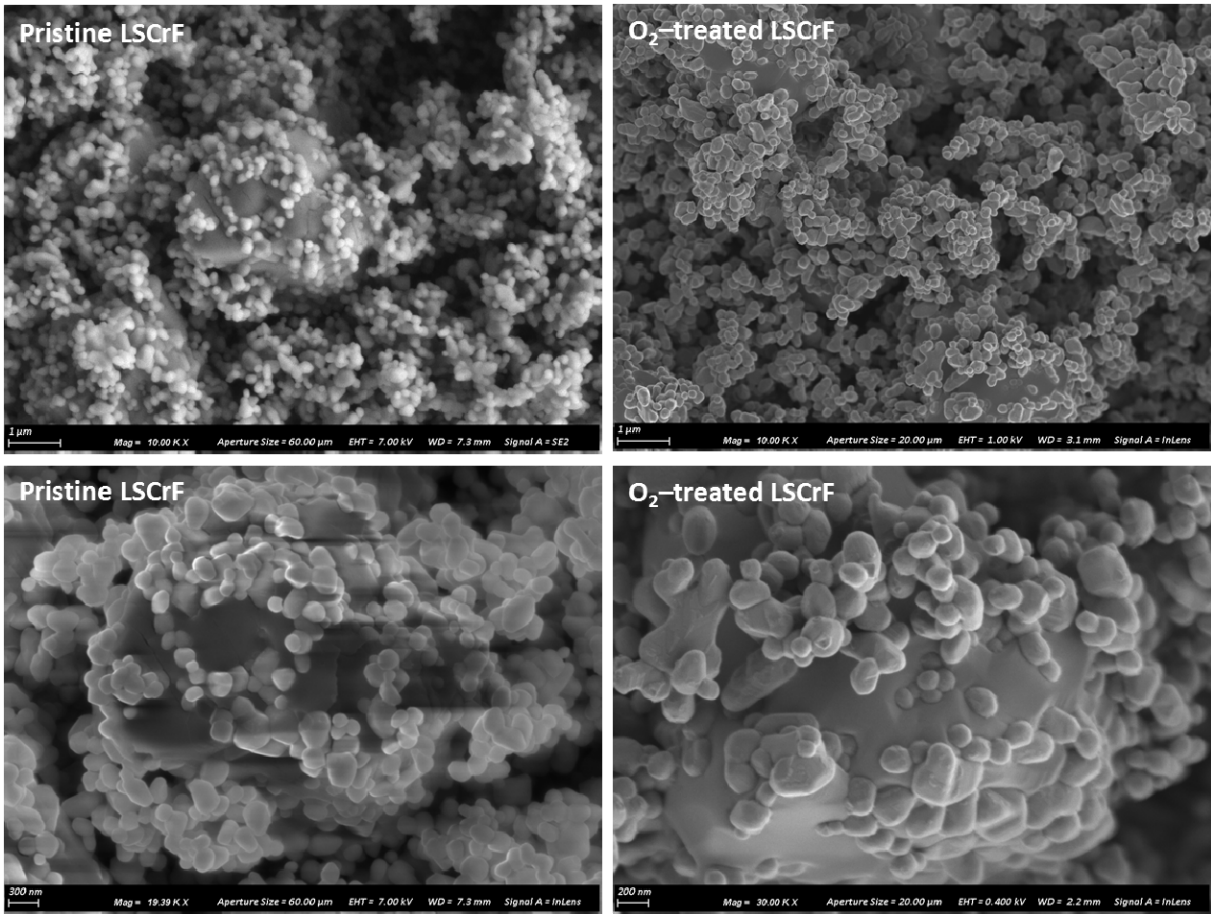

Figure S 6. Characteristic SEM micrographs of the surface of pristine and O_2 –treated LSCrF electrodes, taken in two different magnifications.

Supporting information 8

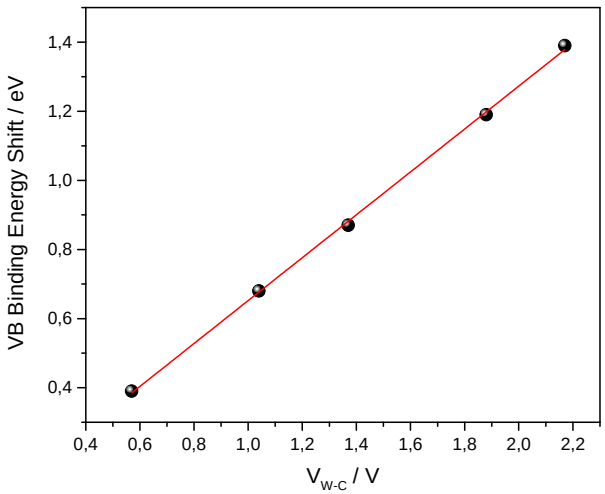

Figure S 7. The evolution of valence band cut-off as a function of the potential (slope: 0.62 eV/V) measured between the counter (Pt) and the working (LSCrF) electrodes under galvanostatic cell operation.

Supporting information 9

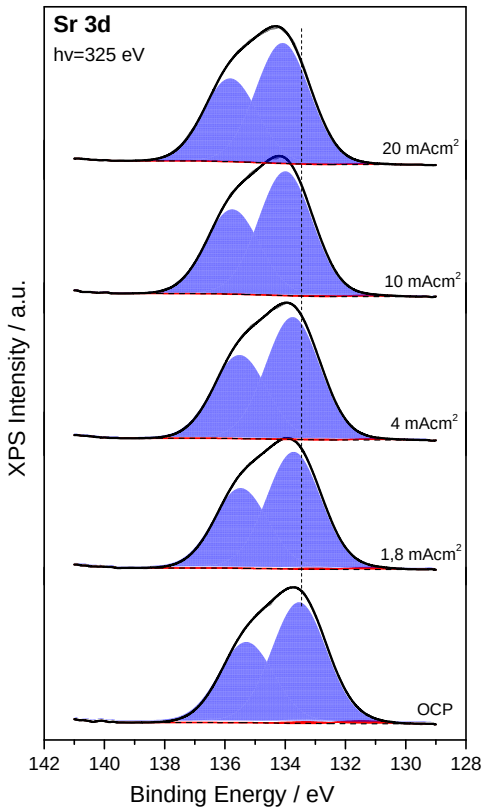

Figure S 8. NAP-XPS Cr 2p spectra (hv = 770 eV) recorded on a LSCrF electrode at different applied current densities (indicated in the figure) under 1 mbar H_2O at 700 °C. The spectra are normalized to the background and offset for clarity.

Supporting information 10

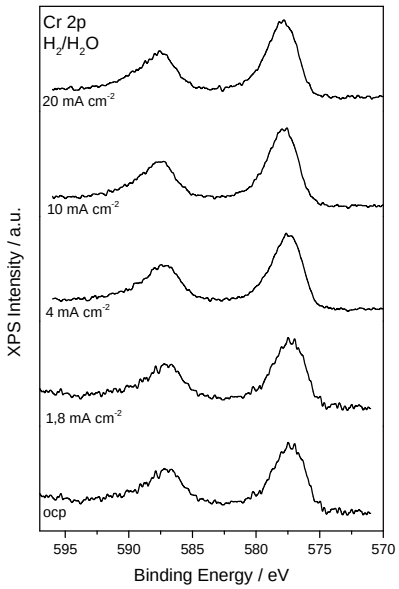

Figure S 9. NAP-XPS Cr 2p spectra (hv = 770 eV) recorded on a LSCrF electrode at different current densities (indicated in the figure) under 1 mbar H_2O/H_2 (1/1) at 700 °C. The spectra are normalized to the background and offset for clarity.

Supporting information 11

$SrCrO_4$ to SrO ratio was calculated from the Cr 2p and Sr 3d NAP-XPS spectra. In particular, the area of the Cr^{6+} component at the Cr 2p was divided by that of Sr 3d peak (only the s-SrO component was detected in this experiment) after proper normalization with the photoemission cross-section and the photon flux intensity. In the case that all the s-SrO signal comes from $SrCrO_4$ compound the $SrCrO_4$/SrO ratio should be equal to 1 (the stoichiometry of Sr and Cr in $SrCrO_4$). $SrCrO_4$/SrO < 1 indicates an excess of s-SrO which did not react with Cr, most probably due to the limited amount of available Cr6+ species.